Accepted Manuscript

http://dx.doi.org/10.1039/C8DT02619J

S. Neuberger, S.P. Culver, H. Eckert, W.G. Zeier, and J. Schmedt auf der Günne. Refinement of the crystal structure of $Li_4P_2S_6$ using NMR crystallography. *Dalton Trans.*, 47:11691--11695, 2018.

Journal Name

ARTICLE

Refinement of the Crystal Structure of $Li_4P_2S_6$ using NMR Crystallography

Received 00th January 20xx,
Accepted 00th January 20xx

DOI: 10.1039/x0xx00000x

www.rsc.org/

Sven Neuberger[a], Sean P. Culver[b], Hellmut Eckert[c,d], Wolfgang G. Zeier[b], Jörn Schmedt auf der Günne[a]

The structure of $Li_4P_2S_6$ was solved, based on a combination of X-ray powder diffraction data, quantum chemical calculations and solid state nuclear magnetic resonance (NMR). Two-dimensional ^{31}P single quantum/double quantum correlation spectra yielded important constraints regarding the space group symmetry allowing the crystal structure to be solved by the Rietveld method. $Li_4P_2S_6$ crystallizes in a trigonal space group with a = 10.51452(6) Å; c = 6.59149(8) Å. The structure contains two distinct $P_2S_6^{4-}$ ions in a 2:1 ratio: in the first one the two P atoms of the hexahypothiophosphate unit are crystallographically distinct, whereas in the second one they are crystallographically identical.

Introduction

Lithium rich thiophosphates are a promising class of ion conductors already in use as electrolytes in solid-state batteries.[1–3] Room temperature ionic conductivities between 10^{-2} and 10^{-3} Scm^{-1} have been measured for the lithium argyrodites Li_6PS_5X (X = Cl, Br),[4] $Li_{10}MP_2S_{12}$ (M = Si, Al, Sn, Ge),[5–9] and several glassy and crystalline Li_2S-P_2S_5 systems such as Li_3PS_4 (thio-LISICON analogues)[10–12] and $Li_7P_3S_{11}$.[13]

Another Li-rich crystalline phase, albeit with very low ionic conductivity, is $Li_4P_2S_6$ ($\sigma = 1.6 \cdot 10^{-10}$ S · cm^{-1} at 300 K).[14] In order to rationalize the low lithium ion mobility of this compound, it is important to understand its crystal structure. Mercier et al. published a disordered crystal structure[15] for $Li_4P_2S_6$, in which all the lithium atoms are stacked in a chain-like fashion between the $P_2S_6^{4-}$ units. The only phosphorus site in this crystal structure is statistically half occupied. Recently, Dietrich et al.[14] published a new structural model that does not show any disorder and therefore contains two crystallographic phosphorus sites.

However, former ^{31}P solid-state nuclear magnetic resonance (NMR) spectroscopy investigations[16,17] contradict those structural models. In this article, we investigate the crystal structure of $Li_4P_2S_6$ synthesized by incongruent crystallization from glassy $Li_4P_2S_7$ using NMR crystallography[18,19], i.e. a combined approach of solid state NMR spectroscopy, X-ray powder diffraction (XRD) and computational techniques. Based on important constraints developed by the solid-state NMR spectra, we propose a new space group symmetry, which corresponds to a superstructure with respect to the previously reported structural model.

Experimental Methods

Synthesis

All starting materials were stored inside a glove box (MBraun, Garching, Germany) under argon atmosphere. All sample preparations were carried out in the same glove box under the same conditions. $Li_4P_2S_6$ was synthesized according to the procedure described by Mercier et al.[15] Red phosphorus (4.36 mmol, 134.9 mg, ACROS Organics, 99.999%), sulfur (8.71 mmol, 279.2 mg, ChemPur, 99.999%) and lithium sulfide (4.36 mmol, 200.0 mg, Alfa Aesar, 99.9%) were thoroughly ground and mixed in an agate mortar and afterwards filled into a graphitized quartz ampoule (8 mm outer diameter). The ampoule was sealed under vacuum ($p = 1.5 \cdot 10^{-2}$ mbar) and heated to 900 °C for 1 h. Afterwards, the ampoule was taken out of the 900 °C hot furnace and quenched in ice water. Subsequently, the ampoule was heated to 450 °C for 16 h.

NMR Spectroscopy

For all the solid-state NMR measurements the ^1H resonance of 1 % $Si(CH_3)_4$ in $CDCl_3$ served as an external secondary reference using the Ξ values for ^{31}P and ^6Li as reported by the IUPAC.[20] The magic angle spinning (MAS) rotors (4 mm, ZrO_2) were packed in a glove box under argon atmosphere. The ^{31}P and ^6Li MAS NMR measurements were carried out on a Bruker Avance II spectrometer at a frequency of 121.50 MHz and 44.17 MHz,

[a] Inorganic Materials Chemistry, University of Siegen, Adolf-Reichwein-Straße 2, 57076 Siegen, Germany
[b] Institute of Physical Chemistry, Justus-Liebig-University Giessen, Heinrich-Buff-Ring 17, D-35392 Giessen, Germany
[c] Institute of Physics in São Carlos, University of São Paulo, Av. Trabalhador Sãocarlense 400, Sao Carlos, SP 13566-590, Brazil
[d] Institute of Physical Chemistry, WWU Münster, Corrensstraße 30, D-48149 Münster, Germany

Electronic Supplementary Information (ESI) available: Details of structural transformations, comparison of the Rietveld refinements of the new structure model, the planar structure model and the Mercier structure model, comparison of the low angle reflections of the Lab X-ray and synchrotron diffraction pattern, DFT optimization of the new structure model and Madelung energies, crystallographic data of the calculated structure, crystallographic information file (CIF). See DOI: 10.1039/x0xx00000x

respectively (B_0 = 7.0 T) with a home-built 4 mm McKay probe at a sample spinning frequency of ν_{rot} = 10 kHz. For the ^{31}P MAS NMR measurement, a repetition delay of 8192 s was used, for the ^{6}Li MAS NMR measurement 80 s were used. For the ^{31}P-^{31}P 2D double-quantum (DQ) - single-quantum (SQ) coherence correlation spectroscopy measurement, the phase tuned PostC7[21,22] sequence was used with a repetition delay of 16 s and a conversion period of 1.6 ms and rotor-synchronized data sampling of the indirect dimension accumulating 16 transients/FID.

X-ray Powder Diffraction and structural transformations

X-ray powder diffraction (XRD) analyses were conducted using a STOE STADI P powder diffractometer (Stoe, Darmstadt, Germany) with Cu $K_{\alpha1}$ radiation (λ = 1.54051 Å). Here a 2Θ range between 10° and 90° with a step size of 0.015° was measured, using a counting time of 180 s per step. Structural transformations by group-subgroup relations of the literature structure of Mercier et al.[15] were done using PowderCell,[23] normalization of structural parameters was done in Platon.[24]

Rietveld Analysis

Rietveld refinements were carried out using the TOPAS academic V4.1[25] and V6.[26] The space groups $P\bar{3}$ (no. 147), $P321$ (no. 150) and $P\bar{3}m1$ (no. 164) were used as starting models. Fit indicators of R_{wp}, R_{exp}, and GOF were used to assess the quality of the refined structural models.[27] The following parameters were initially refined: (1) scale factor, (2) background coefficients using a Chebyshev function with 10 free parameters, (3) peak shape, which was modeled using a modified Thomson–Cox–Hastings pseudo-Voigt function,[28] (4) lattice constants, (5) fractional atomic coordinates of the P and S atoms, (6) isotropic atomic displacement parameters of the P and S atoms, and (7) zero-shift error. Fractional atomic coordinates for the lithium atoms were fixed to the simulated structural values and the atomic displacement parameters for the lithium atoms were fixed to B_{eq} = 5 Å^2.

Results & Discussion

NMR constraints for the crystal structure of $Li_4P_2S_6$

$Li_4P_2S_6$ was analysed by solid-state NMR in order to obtain more information on its crystal structure. The ^{31}P MAS NMR spectrum of $Li_4P_2S_6$ (Fig. 1) features two sharp peaks at δ = 107.3 and 109.2 ppm with a peak area ratio of exactly 1.0:2.0, which can be assigned to the phosphorus atoms of the $P_2S_6^{4-}$ units. Thus, the crystal structure must contain at least two different crystallographic phosphorus orbits (sites). The ^{6}Li MAS NMR spectrum (Fig. 1) of $Li_4P_2S_6$ features two sharp peaks at δ = 0.3 ppm and −0.9 ppm with a peak area ratio of 3.0:1 which fits to the observations of Eckert et al.,[29] who observed an asymmetric peak shape at lower spinning frequencies. Hence, the crystal structure must contain at least four different crystallographic lithium orbits. Further, the new crystal structure may not possess any disorder, as a disordered structure would have caused much broader peaks.

The homonuclear ^{31}P-^{31}P DQ-SQ coherence MAS NMR spectrum of $Li_4P_2S_6$ (Fig. 2) indicates that the signal at 109.2 ppm actually consists of two peaks at 109.3 ppm and 109.1 ppm with almost identical chemical environments and equal intensities. The isotropic chemical shift values of all signals and relaxation times of the ^{31}P signals are listed in Table 1. Therefore, the crystal structure of $Li_4P_2S_6$ must contain not two different crystallographic phosphorus orbits with different multiplicities but three crystallographic orbits with the same multiplicity, in which two sites have a very similar chemical environment. The first peak at 109.3 ppm correlates with the third peak at 107.3 ppm, which means that those two peaks result from two distinct crystallographic phosphorus orbits forming one hexahypothiophosphate unit. The second peak at 109.1 ppm only correlates with itself. Hence this crystallographic phosphorus site forms a hexahypothiophosphate unit with another P atom of the same site. This means that there are two distinct hexahypothiophosphate units in a 2:1 ratio: in the first (majority), the two P atoms are crystallographically different, whereas in the second (minority), the two P atoms are on crystallographically identical sites.

With these constraints, it is possible to look for a new structural model. Given that the electron densities predicted from the Mercier structure reflected the most prominent reflections in the diffractogram, we follow the hypothesis that the true structure can be found by group-subgroup relations, as described by Müller.[30] Thus, several steps of symmetry reduction were carried out from the originally published structure with the space group $P6_3/mcm$ in order to find a proper structure model. The complete group-subgroup graph is shown in the Supporting Information (Fig. S1).

Table 1: Isotropic chemical shift values of the ^{31}P and ^{6}Li signals and relaxation times of the ^{31}P signals

	Peak 1	Peak 2	Peak 3
δ_{iso} (^{31}P) / ppm	109.3(1)	109.1(1)	107.3 (1)
T_1 (^{31}P) / s	1035(4)	1035(4)	1031(4)
δ_{iso} (^{6}Li) / ppm	–0.9(1)	0.3(1)	–

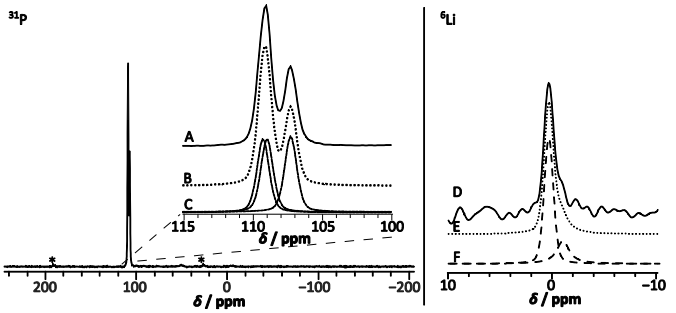

Fig. 1 Experimental ^{31}P and ^{6}Li MAS NMR spectra of $Li_4P_2S_6$ at ν_{rot} = 10 kHz. Spinning sidebands are marked with an asterisk. (A) shows the phosphorus peaks of the experimental ^{31}P MAS NMR spectrum of $Li_4P_2S_6$, (B) shows the simulated ^{31}P spectrum resulting in the simulated peaks with an intensity ratio of 1.0:1.0:1.0 (spectrum (C)). (D) shows the experimental ^{6}Li MAS NMR spectrum of $Li_4P_2S_6$ at ν_{rot} = 10 kHz, (F) shows the ^{6}Li spectrum of two simulated peaks with an peak area ratio of 3.0:1 of spectrum resulting in spectrum (E). Due to the limited resolution of the spectrum, the exact peak area ratio is subject to a bigger uncertainty.

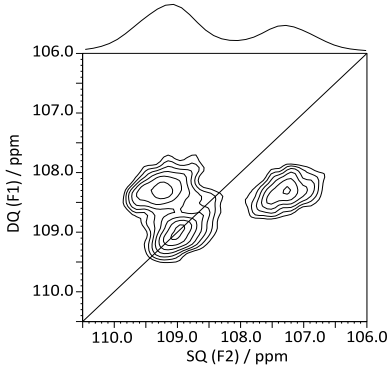

Fig. 2 Homonuclear ^{31}P-^{31}P DQ SQ coherence MAS NMR spectrum of $Li_4P_2S_6$ at ν_{rot} = 10 kHz. Correlation peaks are shown via contour plots. The 1D projection from the one-pulse experiment is plotted on top of the 2D spectrum. The diagonal line (autocorrelation diagonal) refers to the hypothetic peak positions of two isochronous spins.

Finding the right space group

From the 101 possible solutions obtained by symmetry reduction, all substructures with three phosphorus sites show unphysically short internuclear P-P distances (< 1 Å) and therefore do not comply with the experimental requirements.

In order to get an ordered structure with three phosphorus sites forming $P_2S_6^{4-}$ units with the desired symmetry and proper internuclear distances, it is necessary to find a subgroup, which contains six half occupied phosphorus sites, from which three phosphorus sites have to be eliminated. The tree diagrams for all symmetry transformations are shown in Fig. S2-S6. The space group $P\bar{3}m1$, after symmetry reduction of the planar structure model, and all substructures with the space groups $P\bar{3}$ and $P321$, after three steps of symmetry reduction from the Mercier structure model, contain six half-occupied phosphorus sites with different numbers of lithium sites. Additionally, the inversion symmetry is maintained for both space groups. Both structures are depicted in Fig. 3.

For the five solutions in the subgroups $P\bar{3}m1$, $P\bar{3}$ and $P321$, there are four possibilities each, to eliminate the above-mentioned three P-sites to obtain a fully ordered model. Only structure models which have two crystallographically inequivalent $P_2S_6^{4-}$ groups are possible, of which one has two crystallographically equivalent P-atoms and one that has two inequivalent P-atoms. By this reasoning for example planar arrangements can be excluded.

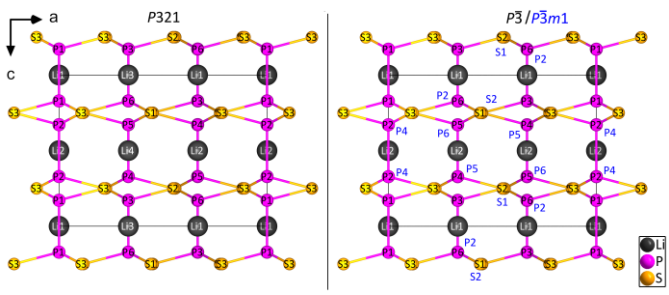

Fig. 3 Structure models for $Li_4P_2S_6$ with space group $P321$ (left) and $P\bar{3}$ and $P\bar{3}m1$ (right) after symmetry reduction from viewing direction *b*. The different alignments of the atom sites for $P\bar{3}m1$ are given with blue atom labels.

In order to determine, which space group and which arrangement fits best to the laboratory X-ray diffraction data, Rietveld refinements were performed using all structure models.

Refinement of the crystal structure

Rietveld refinements of the different arrangements of $P\bar{3}$ converged to fit minima, in which no $P_2S_6^{4-}$ units were present, only planar and pyramidal PS_3 units, which contradicts the NMR data. The calculated X-ray diffraction patterns for all arrangements of the structure model with space group $P\bar{3}m1$ did not show all of the reflexes in the experimental diffractogram.

Rietveld refinements of the different arrangements of $P321$ yielded structures with similar quality factors. Normalization of the crystal structures of those different arrangements revealed that both structures were the same and simply shifted by a fraction of the lattice constant. The structural parameters are listed in Table 2. Additionally, results from DFT calculations and a comparison of calculated Madelung energies are provided in the Supporting Information.

Fig. 4 shows a Rietveld refinement of laboratory X-ray diffraction data of $Li_4P_2S_6$, with the new structural solution in space group $P321$. The refinement leads indeed to a slight, but statistically significant, improvements of the refinement residuals, as compared to the planar structure that was recently presented by Dietrich et al.[14] Deviations in the intensities of some reflections relative to the new structural solution can be explained by merohedral twinning of crystallites and rod disorder. Twinning may also be responsible for identifying a hexagonal space group instead of a trigonal one. The tabulated structural parameters can be found in Table 3. The crystal structure is shown in Fig. 5. The autocorrelation signal at 109.1 ppm of the ^{31}P-^{31}P DQ SQ coherence MAS NMR spectrum can clearly be assigned to the P1 site, while the other both peaks at 109.3 and 107.3 ppm can be assigned to the other two P sites. A comparison of the laboratory X-ray diffraction data refined against both structural models is shown in Fig. S7.

A comparison of the low intensity reflections of the new structural model and the models by Mercier et al.[15] and Dietrich et al.[14] and a comparison regarding the requirements on the crystal structure are shown in Fig. S8 and Table 4. The simulated diffraction pattern for the new structural model includes all reflections, while the other two models do not or only partially include those reflections. In addition, Fig. S9 shows a comparison of the laboratory X-ray diffraction data with the synchrotron diffraction data of the samples prepared by Dietrich et al.[14] The data show that both structures can be easily distinguished by the (101) Miller reflection, that is only present in the structure with space group $P321$. However, the lower crystallinity of the samples measured using synchrotron diffraction leads to a (101) reflection that is being covered by the asymmetry of the beam. Therefore, the (101) reflection cannot be found in poorly crystalline samples, due to the asymmetry, which indeed seems to be the reason for the

incorrect, initial indexing of the $Li_4P_2S_6$ structure to the space group *P*3*m*1.

Table 2: Initial structural parameters of the normalized structure for space group *P*321

Atom	Wyckoff site	*x*	*y*	*z*	Occ.
Space group *P*321 (150) with *a* = *b* = 10.5137 Å and *c* = 6.5918 Å					
Li1	3e	0.6250	0	0	1
Li2	3f	0.6309	0	1/2	1
Li3	3e	0.3170	0	0	1
Li4	3f	0.3290	0	1/2	1
P1	2c	0	0	0.1698	1
P2	2d	1/3	2/3	0.6627	1
P3	2d	1/3	2/3	0.3306	1
S1	6g	0.1084	0.2147	0.2435	1
S2	6g	0.1240	0.5612	0.2554	1
S3	6g	0.4505	0.2249	0.2628	1

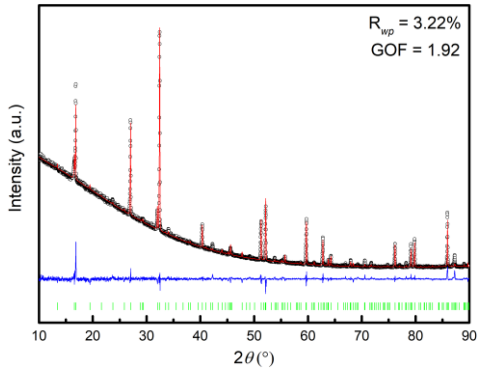

Fig. 4 Rietveld refinement of laboratory X-ray diffraction data of $Li_4P_2S_6$, showing the experimental data (black data points), the fit (red line), the difference profile (blue line) and expected Bragg reflections. The resulting profile residuals are given in the inset.

Table 3: Crystallographic data (atomic coordinates, B_{eq}, and occupancy) of $Li_4P_2S_6$ at room temperature, obtained from Rietveld refinements of X-ray powder data (λ = 1.54051 Å) and isotropic displacement parameters.

$Li_4P_2S_6$ structure from X-ray powder diffraction (space group *P*321, No.150); *a* = 10.51452(6) Å; *c* = 6.59149(8) Å Fit residuals (R_{wp}, R_{exp}, GOF): 3.22, 1.68, 1.92						
Atom	Wyckoff site	*x*	*y*	*z*	Occ.	B_{eq} /Å^2
Li1	3e	0.625	0	0	1.0	5
Li2	3f	0.631	0	0.5	1.0	5
Li3	3e	0.317	0	0	1.0	5
Li4	3f	0.329	0	0.5	1.0	5
P1	2c	0	0	0.170(1)	1.0	2.7(1)
P2	2d	0.333	0.666	0.663(1)	1.0	2.7(1)
P3	2d	0.333	0.666	0.335(1)	1.0	2.7(1)
S1	6g	0.108(6)	0.2165(7)	0.2410(9)	1.0	0.7(1)
S2	6g	0.1221(9)	0.561(8)	0.2500(9)	1.0	0.7(1)
S3	6g	0.4515(7)	0.226(6)	0.255(1)	1.0	0.7(1)

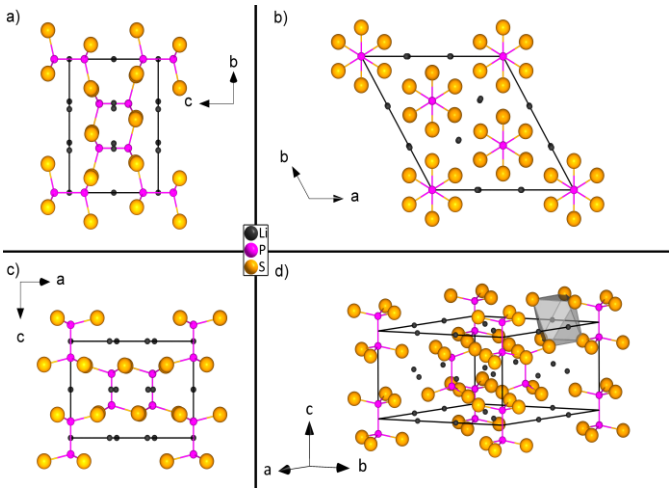

Fig. 5 Crystal structure of $Li_4P_2S_6$ after Rietveld refinement from different viewing directions. a) viewing direction *a*, b) viewing direction *c*, c) viewing direction *b*. d) a side view on the $P_2S_6^{4-}$ units of the crystal structure.

Table 4: Comparison of the different structural models regarding the experimental requirements

	Mercier[15]	Planar[14]	This work
ordered structure	no	no	yes
number of P sites	1	2	3
covers all XRD reflections	no	no	yes
consistent with NMR data	no	no	yes

Conclusions

In conclusion, phase pure $Li_4P_2S_6$ was structurally characterized using an NMR crystallographic approach. With the help of solid state NMR and higher-quality X-ray diffraction data, the structure could be refined in a different space group through the symmetry reduction of a previously published structure model. The new structure model, with space group *P*321, shows a fully ordered structure and accounts for the weak superstructure reflexes observed in the X-ray powder diffractogram. As demonstrated by the present study, the combination of Rietveld refinements, based on constraints developed with solid-state NMR and DFT calculations, represents a powerful approach for addressing complex structural issues in polycrystalline materials.

Conflicts of interest

There are no conflicts to declare.

Acknowledgements

We thank *Dr. Johannes Weber* for helping with computational problems.

References

1 C. Masquelier, *Nat. Mater.*, 2011, **10**, 649.
2 J. Janek and W. G. Zeier, *Nat. Energy*, 2016, **1**, 16141.
3 Y. Kato, S. Hori, T. Saito, K. Suzuki, M. Hirayama, A. Mitsui, M. Yonemura, H. Iba and R. Kanno, *Nat. Energy*, 2016, **1**, 16030.
4 H.-J. Deiseroth, S.-T. Kong, H. Eckert, J. Vannahme, C. Reiner, T. Zaiß and M. Schlosser, *Angew. Chem. Int. Ed.*, 2008, **47**, 755–758.
5 A. Kuhn, O. Gerbig, C. Zhu, F. Falkenberg, J. Maier and B. V. Lotsch, *Phys. Chem. Chem. Phys.*, 2014, **16**, 14669–14674.
6 P. Zhou, J. Wang, F. Cheng, F. Li and J. Chen, *Chem. Commun.*, 2016, **52**, 6091–6094.
7 P. Bron, S. Johansson, K. Zick, J. Schmedt auf der Günne, S. Dehnen and B. Roling, *J. Am. Chem. Soc.*, 2013, **135**, 15694–15697.
8 R. Kanno and M. Murayama, *J. Electrochem. Soc.*, 2001, **148**, A742–A746.
9 N. Kamaya, K. Homma, Y. Yamakawa, M. Hirayama, R. Kanno, M. Yonemura, T. Kamiyama, Y. Kato, S. Hama, K. Kawamoto and A. Mitsui, *Nat. Mater.*, 2011, **10**, 682.
10 K. Homma, M. Yonemura, M. Nagao, M. Hirayama and R. Kanno, *J. Phys. Soc. Jpn.*, 2010, **79**, 90–93.
11 Z. Zhu, I.-H. Chu and S. P. Ong, *Chem. Mater.*, 2017, **29**, 2474–2484.
12 M. Murayama, R. Kanno, Y. Kawamoto and T. Kamiyama, *Solid State Ion.*, 2002, **154-155**, 789–794.
13 H. Yamane, M. Shibata, Y. Shimane, T. Junke, Y. Seino, S. Adams, K. Minami, A. Hayashi and M. Tatsumisago, *Solid State Ion.*, 2007, **178**, 1163–1167.
14 C. Dietrich, M. Sadowski, S. Sicolo, D. A. Weber, S. J. Sedlmaier, K. S. Weldert, S. Indris, K. Albe, J. Janek and W. G. Zeier, *Chem. Mater.*, 2016, **28**, 8764–8773.
15 R. Mercier, J. P. Malugani, B. Fahys, J. Douglande and G. Robert, *J. Solid State Chem.*, 1982, **43**, 151–162.
16 J. Schmedt auf der Günne and H. Eckert, *Proc. Jt. 29th AMPERE-13th ISMAR*, 1998, 1:292–293.
17 J. Schmedt auf der Günne and H. Eckert, *Chem. – Eur. J.*, 1998, **4**, 1762–1767.
18 C. Martineau, *Solid State Nucl. Magn. Reson.*, 2014, **63-64**, 1–12.
19 D. L. Bryce, *IUCrJ*, 2017, **4**, 350–359.
20 R. K. Harris, E. D. Becker, S. M. Cabral de Menezes, P. Granger, R. E. Hoffman and K. W. Zilm, *Pure Appl. Chem.*
21 M. Hohwy, H. J. Jakobsen, M. Edén, M. H. Levitt and N. C. Nielsen, *J. Chem. Phys.*, 1998, **108**, 2686–2694.
22 J. Weber, M. Seemann and J. Schmedt auf der Günne, *Solid State Nucl. Magn. Reson.*, 2012, **43-44**, 42–50.
23 W. Kraus and G. Nolze, *PowderCell*, Federal Institute for Materials Research and Testing, Berlin, 2000.
24 A. L. Spek, *Acta Crystallogr. D Biol. Crystallogr.*, 2009, **65**, 148–155.
25 A. A. Coelho, *TOPAS-Academic V4.1*, Coelho Software, Brisbane, 2007.
26 A. A. Coelho, *TOPAS-Academic V6*, Coelho Software, Brisbane, 2017.
27 R. A. Young, Ed., *The Rietveld Method*, Oxford University Press, Oxford, New York, 1995.
28 P. Thompson, D. E. Cox and J. B. Hastings, *J. Appl. Crystallogr.*, 1987, **20**, 79–83.
29 H. Eckert, Z. Zhang and J. H. Kennedy, *Chem. Mater.*, 1990, **2**, 273–279.
30 H. Wondratschek and U. Müller, *International Tables for Crystallography, Volume A1, 2nd Edition, Symmetry Relations between Space Groups*, Wiley, 2010.